

Article

# Efficient Catalytic Dehydration of High-Concentration 1-Butanol with Zn-Mn-Co Modified $\gamma$ -Al<sub>2</sub>O<sub>3</sub> in Jet Fuel Production

Jing Wu <sup>1</sup>, Hong-Juan Liu <sup>1</sup>, Xiang Yan <sup>1</sup>, Yu-Jie Zhou <sup>1</sup>, Zhang-Nan Lin <sup>1</sup>, Shuo Mi <sup>1</sup>, Ke-Ke Cheng <sup>2,\*</sup> and Jian-An Zhang <sup>1,\*</sup>

<sup>1</sup> Institute of Nuclear and New Energy Technology, Tsinghua University, Beijing 100084, China; wj6387@163.com (J.W.); liuhongjuan@mail.tsinghua.edu.cn (H.-J.L.); yanxiangwudi@126.com (X.Y.); zhoyuj@mail.tsinghua.edu.cn (Y.-J.Z.); linzhangnan1@163.com (Z.-N.L.); millerevol@aliyun.com (S.M.)

<sup>2</sup> School of Chemical Engineering and Energy Technology, Dongguan University of Technology, Dongguan 523808, China

\* Correspondence: chengkeke@dgut.edu.cn (K.-K.C.); zhangja@tsinghua.edu.cn (J.-A.Z.)

Received: 14 November 2018; Accepted: 11 January 2019; Published: 16 January 2019



**Abstract:** It is important to develop full-performance bio-jet fuel based on alternative feedstocks. The compound 1-butanol can be transformed into jet fuel through dehydration, oligomerization, and hydrogenation. In this study, a new catalyst consisting of Zn-Mn-Co modified  $\gamma$ -Al<sub>2</sub>O<sub>3</sub> was used for the dehydration of high-concentration 1-butanol to butenes. The interactive effects of reaction temperature and butanol weight-hourly space velocity (WHSV) on butene yield were investigated with response surface methodology (RSM). Butene yield was enhanced when the temperature increased from 350 °C to 450 °C but it was reduced as WHSV increased from 1 h<sup>-1</sup> to 4 h<sup>-1</sup>. Under the optimized conditions of 1.67 h<sup>-1</sup> WHSV and 375 °C reaction temperature, the selectivity of butenes achieved 90%, and the conversion rate of 1-butanol reached 100%, which were 10% and 6% higher, respectively, than when using unmodified  $\gamma$ -Al<sub>2</sub>O<sub>3</sub>. The Zn-Mn-Co modified  $\gamma$ -Al<sub>2</sub>O<sub>3</sub> exhibited high stability and a long lifetime of 180 h, while the unmodified  $\gamma$ -Al<sub>2</sub>O<sub>3</sub> began to deactivate after 60 h. Characterization with X-ray diffraction (XRD), nitrogen adsorption-desorption, pyridine temperature-programmed desorption (Py-TPD), pyridine adsorption IR spectra, and inductively coupled plasma atomic emission spectrometry (ICP-AES), showed that the crystallinity and acid content of  $\gamma$ -Al<sub>2</sub>O<sub>3</sub> were obviously enhanced by the modification with Zn-Mn-Co, and the loading amounts of zinc, manganese, and cobalt were 0.54%, 0.44%, and 0.23%, respectively. This study provides a new catalyst, and the results will be helpful for the further optimization of bio-jet fuel production with a high concentration of 1-butanol.

**Keywords:** 1-butanol; gamma alumina; catalyst; dehydration; bio-jet fuel

## 1. Introduction

Recently, the consumption of jet fuel has been increasing due to the development of the aviation industry, which has resulted in many environmental problems and energy security issues. Therefore, developing full-performance bio-jet fuel based on alternative feedstocks is urgent. The compound 1-butanol can be transformed into jet fuel through dehydration, oligomerization, and hydrogenation [1,2]. Efficient catalytic dehydration of 1-butanol to butenes is the first step and an important guarantee for further processing.

Considerable researches have focused on the conversion of sugars obtained from biomass to 1-butanol, where sugars can be fermented to ‘acetone-butanol-ethanol’ (ABE) using *Clostridium acetobutylicum* or *Clostridium beijerinckii* [3,4]. Fermented 1-butanol can be separated from the fermentation broth

by techniques such as gas-stripping, distillation, membrane separation, and extraction. Generally, fermented 1-butanol is separated into an aqueous phase with 7.7 wt % 1-butanol and an organic phase including 79.9 wt % bio-butanol and 20.1 wt % water at 20 °C. Lin et al. used fed-batch fermentation coupled with gas-stripping for 1-butanol production, and an aqueous phase (84.64 g/L 1-butanol) and an organic phase (624 g/L 1-butanol) were obtained [5]. Xue et al. developed a two-stage gas-stripping technology coupled with 1-butanol fermentation, and the concentrations of 1-butanol in the organic phase and aqueous phase were 612.3–623.3 g/L and 91.3–101.3 g/L, respectively; the aqueous phase was heated and gas-stripped again to concentrate 1-butanol [6,7]. Some researches focusing on the dehydration of low-concentration 1-butanol [8] and pure 1-butanol [9,10] have been reported. However, using a high-concentration 1-butanol solution as feedstock seems more economical than using low-concentration 1-butanol or pure 1-butanol, because low-concentration 1-butanol leads to low productivity of butene and the pure 1-butanol needs to be separated further. Unfortunately, the dehydration of high-concentration 1-butanol solutions is seldom studied.

$\gamma$ -Al<sub>2</sub>O<sub>3</sub> and zeolites show high activity in the alcohol catalytic dehydration reaction. Zeolites with 10-ring unidirectional channels such as Theta-1 and ZSM-23 can efficiently catalyze butanol to butenes, but by-products would be produced such as propylene and C5 olefins [11]. When using  $\gamma$ -Al<sub>2</sub>O<sub>3</sub> as a catalyst, the composition of the products is relatively easier to control, and the product distribution depends on the process temperature and strength of catalyst acidity [12,13]. It has been proven that there is more dibutylether than butenes in the products when the reaction temperature is below 310 °C, and, as the temperature rises, butenes supersede dibutylether [14]. Transition metal catalysts such as cobalt [15,16], manganese, iron [17], nickel [18], and zinc oxides [19] are often utilized for the alcohol dehydration reaction. Metal-loaded catalysts with high catalytic activity and low cost are more adaptable to industrialization requirements. Osman reported that Cu/ $\gamma$ -Al<sub>2</sub>O<sub>3</sub> showed a high degree of activity and stability in a catalytic methanol dehydration reaction [20]. Said used phosphotungstic acid-supported  $\gamma$ -Al<sub>2</sub>O<sub>3</sub> to catalyze the dehydration of ethanol to diethyl ether. The results indicated that the catalytic performance of supported catalysts was correlated with the strong and intermediate Brønsted acid sites due to the presence of Keggin structure and tungsten oxide [21].

In this study, Zn-Mn-Co modified  $\gamma$ -Al<sub>2</sub>O<sub>3</sub> was prepared, and the catalytic performance of 1-butanol dehydration to butenes was investigated with 620 g/L 1-butanol as the raw material. This concentration of raw material is more consistent with the concentration range of bio-butanol separated from the fermentation broth. The experiments were designed by the central composite design method for optimizing the dehydration process of 1-butanol with respect to temperature (350–450 °C) and WHSV (1.0–4.0) and maximizing butene yield. This study provides a new catalyst, and the results have great significance for the goal of reducing the production cost of bio-jet fuel from 1-butanol.

## 2. Results and Discussion

### 2.1. Catalyst Characterization

The XRD pattern of  $\gamma$ -Al<sub>2</sub>O<sub>3</sub> and Zn-Mn-Co modified  $\gamma$ -Al<sub>2</sub>O<sub>3</sub> are shown in Figure 1. The position of the diffraction peaks of the modified sample was well matched with that of the original sample, which indicated the modification of Zn-Mn-Co had no effects on the crystalline phase of  $\gamma$ -Al<sub>2</sub>O<sub>3</sub>. The intensity of the diffraction peaks became stronger, which suggested that the crystallinity of Zn-Mn-Co modified  $\gamma$ -Al<sub>2</sub>O<sub>3</sub> was higher than that of  $\gamma$ -Al<sub>2</sub>O<sub>3</sub>. The improvement of crystallinity may be attributed to the fact that zinc, manganese, and cobalt formed a spinel solid solution with  $\gamma$ -Al<sub>2</sub>O<sub>3</sub>, which improved the stability of the catalyst in the reaction environment with water [22]. Zinc, manganese, and cobalt oxides were not detected in the spectra, showing that zinc, manganese, and cobalt were highly dispersed on the catalyst surface. Research has suggested that manganese ions play an important role in improving the dispersion of other metal ions [23]. To verify whether metal ions were loaded onto  $\gamma$ -Al<sub>2</sub>O<sub>3</sub>, the metal loadings of the modified catalyst were measured by

the inductively coupled plasma atomic emission spectrometry (ICP-AES) method, and the loading amounts of zinc, manganese, and cobalt were 0.54%, 0.44%, and 0.23%, respectively.

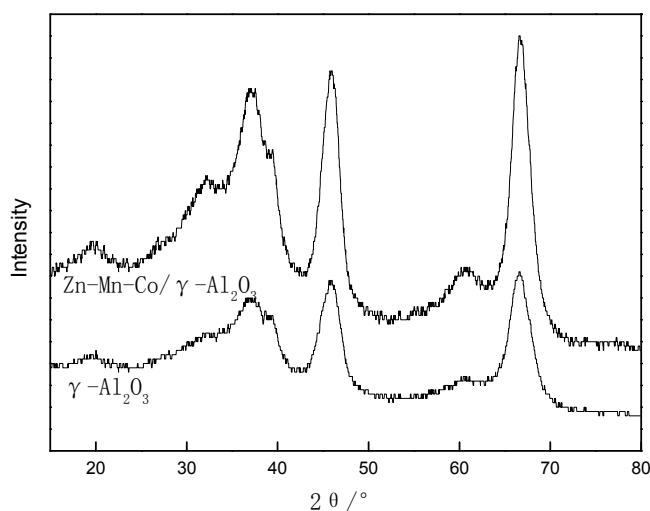


**Figure 1.** X-ray diffraction patterns of  $\gamma$ - $\text{Al}_2\text{O}_3$  and Zn-Mn-Co modified  $\gamma$ - $\text{Al}_2\text{O}_3$ .

Figure 2 shows the nitrogen adsorption–desorption isotherms at liquid nitrogen temperature (77 K) for  $\gamma$ - $\text{Al}_2\text{O}_3$  and Zn-Mn-Co modified  $\gamma$ - $\text{Al}_2\text{O}_3$  samples. Both of the isotherms belong to type IV, and the close hysteresis loops were classified as  $\text{H}_3$  [24]. The specific surface areas, average pore size, and total pore volume of the catalysts are presented in Table 1. The specific surface area of Zn-Mn-Co/ $\gamma$ - $\text{Al}_2\text{O}_3$  was smaller than that of  $\gamma$ - $\text{Al}_2\text{O}_3$ , and the total pore volume was reduced by 15% after modification. However, the average pore radius had a slight increase. This may be due to the modification of the metal ions: some of the micropores were blocked. Figure 3 shows the pore size distribution and cumulative pore volume obtained for the catalysts. The pore sizes of both catalysts were mainly distributed in the range of 5–20 nm. The number of micropores in the modified catalyst was less than that in the original sample, which further proved that the modification of metal ions blocked some of the micropores.

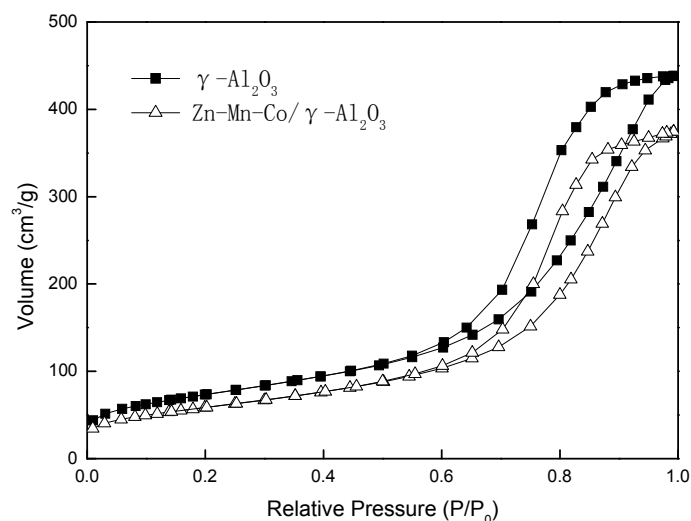


**Figure 2.** Cryogenic nitrogen adsorption-desorption isotherms for  $\gamma$ - $\text{Al}_2\text{O}_3$  and Zn-Mn-Co modified  $\gamma$ - $\text{Al}_2\text{O}_3$ .

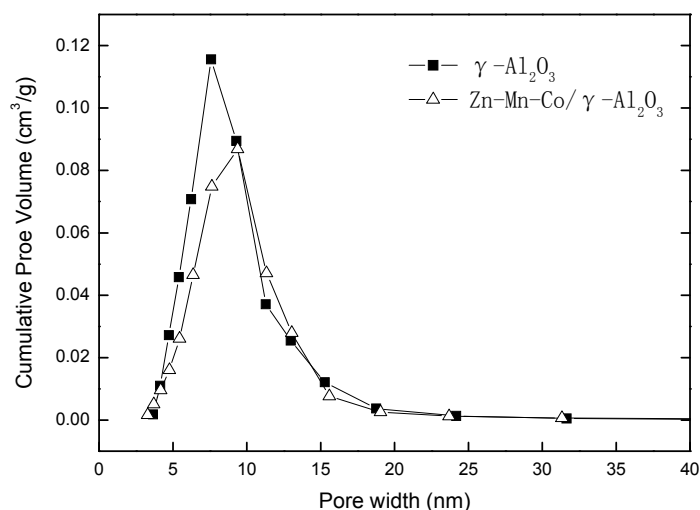


**Figure 3.** Pore size distribution patterns of  $\gamma\text{-Al}_2\text{O}_3$  and Zn-Mn-Co modified  $\gamma\text{-Al}_2\text{O}_3$ .

**Table 1.** Textural properties of the catalysts.

Catalyst	$S_{\text{BET}}$ (m <sup>2</sup> /g)	$V_{\text{ad}}$ (cm <sup>3</sup> /g)	$r$ (nm)
$\gamma\text{-Al}_2\text{O}_3$	264.46	0.67	10.14
Zn-Mn-Co/ $\gamma\text{-Al}_2\text{O}_3$	211.70	0.57	10.72

Note.  $S_{\text{BET}}$  is the Brunner-Emmet-Teller (BET) specific surface area,  $V_{\text{ad}}$  is the cumulative volume of pores,  $r$  is the average pore radius.

The catalytic efficiency of the catalyst is intensively affected by the surface acid sites [8]. In general, most Lewis acids react with water before reacting with the substrate in the presence of water, which results in the deactivation of the catalyst. However, it has been well established that surface Lewis acid sites of alumina catalyze the dehydration of alcohols. Phung et al. reported that the activity of alumina was observed in the dehydration of ethanol (in which water is a reaction product) because of its high surface acidity. Lewis acidity does not require dehydroxylation if the basic substrates can displace water. Substrates that have sufficient basicity to compete with water can also be activated by alumina in the presence of water [14,25].

The pyridine temperature-programmed desorption (Py-TPD) profiles of  $\gamma\text{-Al}_2\text{O}_3$  and Zn-Mn-Co modified  $\gamma\text{-Al}_2\text{O}_3$  are shown in Figure 4. The desorption peak at 200 °C was enhanced after modification, which proved that there were more weak acid sites on Zn-Mn-Co modified  $\gamma\text{-Al}_2\text{O}_3$ . A weak desorption peak appeared at 390 °C, indicating the increase of strong acid sites. The surface acidity values of  $\gamma\text{-Al}_2\text{O}_3$  and Zn-Mn-Co modified  $\gamma\text{-Al}_2\text{O}_3$  were quantified by pyridine adsorption IR spectra (Figure 5 and Table 2). The bands distinguished at 1620 cm<sup>-1</sup> were assigned to pyridine coordinated to tetrahedral and octahedral Al<sup>3+</sup>. The area of the 19b band at 1451 cm<sup>-1</sup> was used to quantify the total amount of Lewis acid sites (LAS) using its molar adsorption coefficient ( $\epsilon = 1.5 \text{ cm}^2/\mu\text{mol}$ ) [10,26–28]. The amount of LAS is given in Table 3. The acidic concentration of total acidity and the strong LAS were measured at 200 °C and 300 °C, respectively. After being modified by zinc, manganese, and cobalt, the total acid content of the catalyst increased by about 10.5%.

**Table 2.** Amount of the Lewis acid sites on the catalysts. LAS, Lewis acid sites.

Catalyst	Weak LAS ( $\mu\text{mol/g}$ )	Strong LAS ( $\mu\text{mol/g}$ )
$\gamma\text{-Al}_2\text{O}_3$	240.8	153.8
Zn-Mn-Co/ $\gamma\text{-Al}_2\text{O}_3$	266.2	170.2

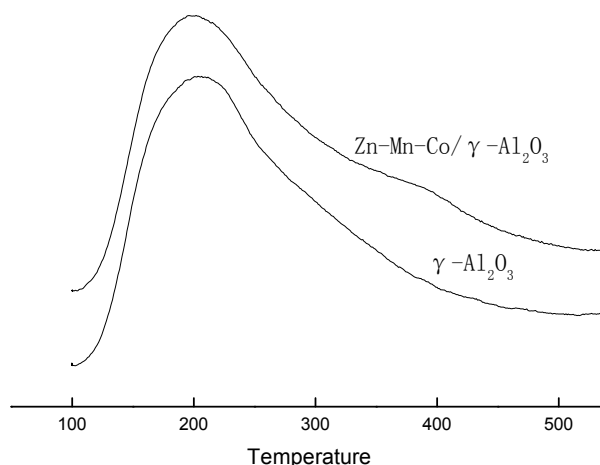


**Figure 4.** The pyridine temperature-programmed desorption (Py-TPD) profiles of  $\gamma$ - $\text{Al}_2\text{O}_3$  and Zn-Mn-Co modified  $\gamma$ - $\text{Al}_2\text{O}_3$ .

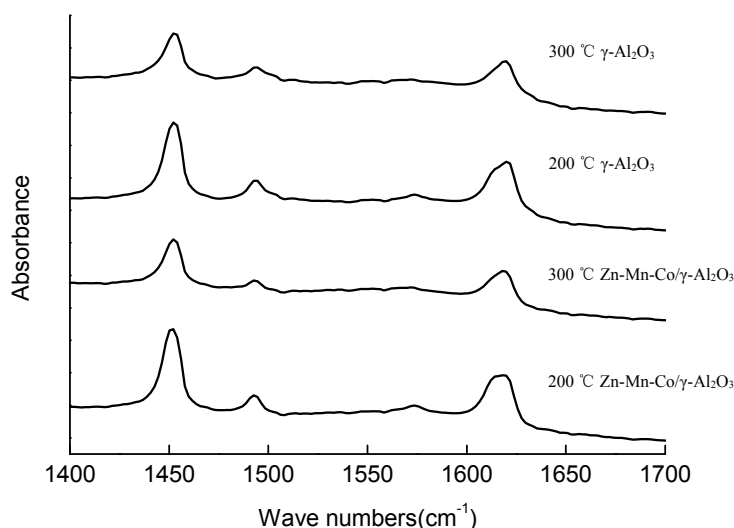


**Figure 5.** The Py-IR profiles of  $\gamma$ - $\text{Al}_2\text{O}_3$  and Zn-Mn-Co modified  $\gamma$ - $\text{Al}_2\text{O}_3$ .

## 2.2. Catalytic Activity of $\gamma$ - $\text{Al}_2\text{O}_3$ and Zn-Mn-Co/ $\gamma$ - $\text{Al}_2\text{O}_3$

The catalytic activity of  $\gamma$ - $\text{Al}_2\text{O}_3$  and Zn-Mn-Co/ $\gamma$ - $\text{Al}_2\text{O}_3$  was investigated at different reaction temperatures (Tables 3 and 4) and WSHV (Tables 5 and 6), with a reaction time of 6 h. The higher reaction temperature had positive effects on the conversion of 1-butanol and the selectivity of butenes, but a too high reaction temperature worked against the selectivity of butenes. The conversion rates of 1-butanol were 71.21% and 82.63% when the reaction temperature was 300 °C and 350 °C, respectively, with  $\gamma$ - $\text{Al}_2\text{O}_3$  as a catalyst, and increased by 12.82% and 15.27% when Zn-Mn-Co/ $\gamma$ - $\text{Al}_2\text{O}_3$  was employed. When the reaction temperature increased from 300 °C to 450 °C, the selectivity of butenes increased to a maximum and then decreased. The highest selectivity of butenes (96.24%) was obtained at the reaction temperature of 400 °C when using Zn-Mn-Co/ $\gamma$ - $\text{Al}_2\text{O}_3$  as the catalyst. A lower reaction temperature led to the formation of dibutyl ether (DBE) and butene, which increased with the increase of the temperature. When the reaction temperature was 450 °C, there was no DBE formation, and some other hydrocarbons such as methane, ethylene, and propylene appeared. Furthermore, the selectivity of butene isomers was strongly influenced by the reaction temperature. More 1-butene was formed at a lower temperature, and higher temperatures led to increased isomerization of 1-butene.

The conversion of 1-butanol dropped rapidly with the increase of WSHV. When the WSHV increased from 1  $\text{h}^{-1}$  to 4  $\text{h}^{-1}$ , the conversion rate of 1-butanol decreased from 98.01% to 51.04% with  $\gamma$ - $\text{Al}_2\text{O}_3$  as the catalyst. The same trend was obtained when the reaction was catalyzed by

Zn-Mn-Co/ $\gamma$ -Al<sub>2</sub>O<sub>3</sub>, and the conversion of 1-butanol was much higher than that when  $\gamma$ -Al<sub>2</sub>O<sub>3</sub> was used as the catalyst. With the increase of WHSV from 1 h<sup>-1</sup> to 4 h<sup>-1</sup>, the proportion of 1-butene in the product increased, and the proportion of butylene isomers decreased. WHSV had little effect on the total selectivity of butenes, which was about 80% and 90% when using  $\gamma$ -Al<sub>2</sub>O<sub>3</sub> and Zn-Mn-Co/ $\gamma$ -Al<sub>2</sub>O<sub>3</sub>, respectively.

The catalytic performance of Zn-Mn-Co/ $\gamma$ -Al<sub>2</sub>O<sub>3</sub> was much better than that of  $\gamma$ -Al<sub>2</sub>O<sub>3</sub>. The high conversion rate of 1-butanol and the selectivity of butenes indicated that Zn-Mn-Co/ $\gamma$ -Al<sub>2</sub>O<sub>3</sub> exhibited excellent activity at low temperature. Zinc, manganese, and cobalt oxides exhibited high activity in alcohol dehydration, as already proven [15–17,29]. The modification of metal ions improved the acidity of the catalyst, and the Lewis acid sites played an important role in the catalytic dehydration of alcohols [30]. A synergistic effect between different metal ions and catalyst carriers improved the catalytic efficiency [23,31].

**Table 3.** Catalytic properties of  $\gamma$ -Al<sub>2</sub>O<sub>3</sub> at different temperatures. DBE, dibutyl ether.

Temperature (°C)	Conversion of 1-Butanol (%)	Selectivity of Butenes (%)					Selectivity of DBE (%)	Other Hydrocarbons (%)
		1-	Trans-	Cis-	Iso-	Total		
300	71.21	65.72	3.87	6.96	0.77	77.32	21.88	-
350	82.63	63.18	7.32	9.61	1.76	81.87	16.76	0.43
400	98.56	56.97	17.13	12.29	2.61	89.00	6.74	2.16
450	100	47.15	20.06	17.54	2.94	87.69	-	10.43

Note: The weight-hourly space velocity (WHSV) was 2.0 h<sup>-1</sup>.

**Table 4.** Catalytic properties of Zn-Mn-Co/ $\gamma$ -Al<sub>2</sub>O<sub>3</sub> at different temperatures.

Temperature (°C)	Conversion of 1-Butanol (%)	Selectivity of Butenes (%)					Selectivity of DBE (%)	Other Hydrocarbons (%)
		1-	Trans-	Cis-	Iso-	Total		
300	80.34	65.11	5.70	9.77	0.82	81.39	17.21	-
350	95.25	64.67	9.59	12.98	1.25	88.49	9.35	0.51
400	100	57.79	20.45	15.13	2.87	96.24	-	2.59
450	100	33.62	25.05	24.29	3.77	86.73	-	11.77

Note: The WHSV was 2.0 h<sup>-1</sup>.

**Table 5.** Catalytic properties of  $\gamma$ -Al<sub>2</sub>O<sub>3</sub> at different WHSV.

WHSV (h <sup>-1</sup> )	Conversion of 1-Butanol (%)	Selectivity of Butenes (%)					Selectivity of DBE (%)	Other Hydrocarbons (%)
		1-	Trans-	Cis-	Iso-	Total		
1	98.01	55.58	11.21	11.05	2.48	80.32	17.89	0.37
2	82.63	63.18	7.31	9.62	1.76	81.87	16.76	0.43
3	68.56	68.69	4.82	6.70	0.83	81.04	17.22	0.39
4	51.04	70.75	4.28	4.53	0.13	79.69	18.52	0.32

Note: The reaction temperature was 350 °C.

**Table 6.** Catalytic properties of Zn-Mn-Co/ $\gamma$ -Al<sub>2</sub>O<sub>3</sub> at different WHSV.

WHSV (h <sup>-1</sup> )	Conversion of 1-Butanol (%)	Selectivity of Butenes (%)					Selectivity of DBE (%)	Other Hydrocarbons (%)
		1-	Trans-	Cis-	Iso-	Total		
1	100	60.60	11.58	15.29	2.90	90.37	8.05	0.48
2	95.25	64.67	9.59	12.98	1.25	88.49	9.35	0.51
3	79.45	72.65	7.16	9.69	0.74	90.24	8.87	0.41
4	65.49	74.97	5.74	8.10	0.36	89.17	9.01	0.48

Note: The reaction temperature was 350 °C.

### 2.3. Optimization of Temperature and WHSV for Butanol Dehydration

To optimize the temperature and WHSV of the 1-butanol dehydration process, experiments were performed in accordance with the conditions listed in Table 7, which was designed by a central

composite design. The values of butene yield ( $Y$ ) obtained in the 1-butanol dehydration experiments at different temperatures and WHSV are shown in Table 7. The results of ANOVA for a fitted quadratic polynomial model are shown in Table 8. The “Model F-value” of 642.51 and the lowest  $p$  value of less than 0.0001 implied that the model was highly significant and there was only a 0.01% chance that a “Model F-value” this large could occur because of noise. The value of  $R^2$  for  $Y$  was 0.9978. Butene yield was significantly affected by reaction temperature and WHSV, which could be deduced from the higher absolute value of  $F$  and the lower  $p$  value (Table 8). The yield of butanol can be predicted by the following equation:

$$Y = -462.49961 + 2.91441X_1 - 30.82659X_2 + 0.067214 X_1X_2 - 0.00374651 X_1^2 - 0.66761X_2^2, \quad (1)$$

where  $X_1$ ,  $X_2$  are the temperature and WHSV, respectively.

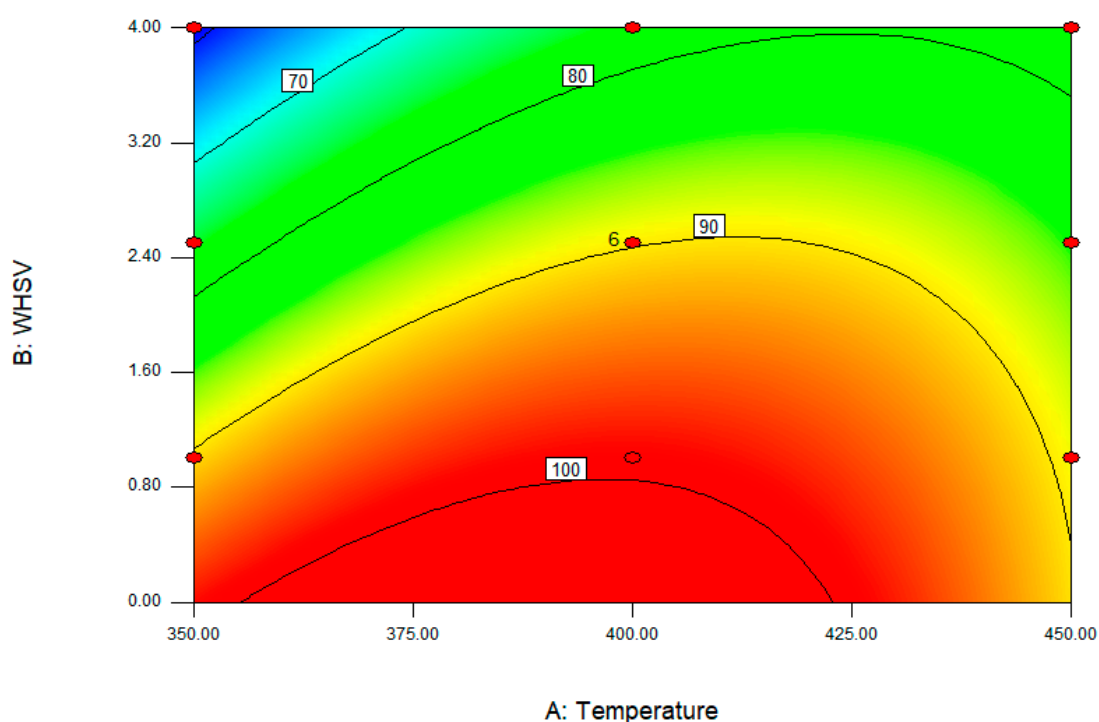
$X_1X_2$  was significant, suggesting that temperature and WHSV interacted. Figure 6 shows the response surface diagram of temperature and WHSV interactions for the total yield of butenes. Butene yield was enhanced as the temperature increased but reduced as WHSV increased. The temperature and WHSV were optimized by the model with the hypothetical conditions of minimum temperature, maximum WHSV, and maximum butene selectivity. The optimum conditions were found to be 375.78 °C and 1.67 h<sup>-1</sup> of WHSV and, under the optimum conditions, the predicted value of total yield of butenes was 92.61%. In a real catalytic reaction of 1-butanol dehydration, the total yield of butenes was 90% at optimum conditions, and the conversion of 1-butanol reached 100%, which were 10% and 6% higher than that when using unmodified  $\gamma$ -Al<sub>2</sub>O<sub>3</sub> in the first 60 h of the reaction. After 60 h of reaction, the unmodified  $\gamma$ -Al<sub>2</sub>O<sub>3</sub> deactivated rapidly, while the Zn-Mn-Co modified  $\gamma$ -Al<sub>2</sub>O<sub>3</sub> showed high stability and long life (Figure 7). Rehydration of  $\gamma$ -Al<sub>2</sub>O<sub>3</sub> is the main reason of deactivation in the presence of water. The rehydration of  $\gamma$ -Al<sub>2</sub>O<sub>3</sub> results in a decrease of the crystallinity of the catalyst and in a significant decrease in the specific surface area of the catalyst [32]. In addition, there is a higher level of by-products of DBE generated with  $\gamma$ -Al<sub>2</sub>O<sub>3</sub> as the catalyst. The DBE may be adsorbed on the surface of the catalyst which leads to the decrease of catalytic efficiency and deactivation of  $\gamma$ -Al<sub>2</sub>O<sub>3</sub>. The crystallinity of  $\gamma$ -Al<sub>2</sub>O<sub>3</sub> was enhanced after modification by Zn-Mn-Co (Figure 1), which improves the stability of the catalyst in the reaction environment with water [22]. The enhancement of surface acidity reduces DBE formation, which also prolongs the life of the catalyst.

**Table 7.** Central composite design and experimental results obtained with Zn-Mn-Co modified  $\gamma$ -Al<sub>2</sub>O<sub>3</sub>.

Run	Temperature (°C)	WHSV (h <sup>-1</sup> )	Butenes Yield (%)
1	400	2.5	90.15
2	400	2.5	90.54
3	350	4.0	58.80
4	450	4.0	77.64
5	400	2.5	89.79
6	450	1.0	89.23
7	350	1.0	90.57
8	400	2.5	89.96
9	400	4.0	77.21
10	350	2.5	76.31
11	400	1.0	99.33
12	400	2.5	89.82
13	450	2.5	84.43
14	400	2.5	88.26

**Table 8.** Analysis of variance for fitted quadratic polynomial model for total yield of butenes.

Source	Sum of Squares	F Value	p-Value Prob > F
Model	1240.91	642.51	<0.0001
X <sub>1</sub> (Temperature)	108.98	282.14	<0.0001
X <sub>2</sub> (WHSV)	715.32	1851.86	<0.0001
X <sub>1</sub> X <sub>2</sub>	101.65	263.15	<0.0001
X <sub>1</sub> X <sub>1</sub>	239.26	619.40	<0.0001
X <sub>2</sub> X <sub>2</sub>	6.15	15.93	<0.0052
Residual	2.70		
Lack of Fit	0.58	0.36	0.7855
Pure Error	2.13		
Cor Total	1268.49		

**Figure 6.** Contour plot of the combined effects of temperature and WHSV on butenes yield obtained with Zn-Mn-Co modified  $\gamma$ -Al<sub>2</sub>O<sub>3</sub>.

The application of  $\gamma$ -Al<sub>2</sub>O<sub>3</sub> for the dehydration of 1-butanol has been reported, and the process temperature appeared to play a decisive role in the distribution of olefins and ethers in the products [12]. The proportion of ethers in the product was larger than that of olefin when the reaction temperature was below 300 °C, and olefin superseded ethers with an increasing temperature [13]. The range of reaction temperature in this study was 350–450 °C, and the main products were butenes, which is consistent with the literature. WHSV mainly affected the retention time of 1-butanol in the catalyst micro-reactor system, and high WHSV was not conducive to the adsorption of butanol by a catalyst, which resulted in a decline of the conversion rate of 1-butanol. Zinc, manganese, and cobalt oxides exhibited excellent catalytic activity in the dehydration reaction of alcohol [15–17] and they are also used as active components to be loaded onto a catalyst carrier [16,19]. In this study, zinc, manganese, and cobalt were loaded onto  $\gamma$ -Al<sub>2</sub>O<sub>3</sub>, and the modified catalyst showed superior catalytic activity, which was attributed to the catalytic ability of the active components and the increase of the catalyst's acidity. In addition, the enhancement of the crystallinity and acidity of the catalyst made it stable and gave it a long lifetime.

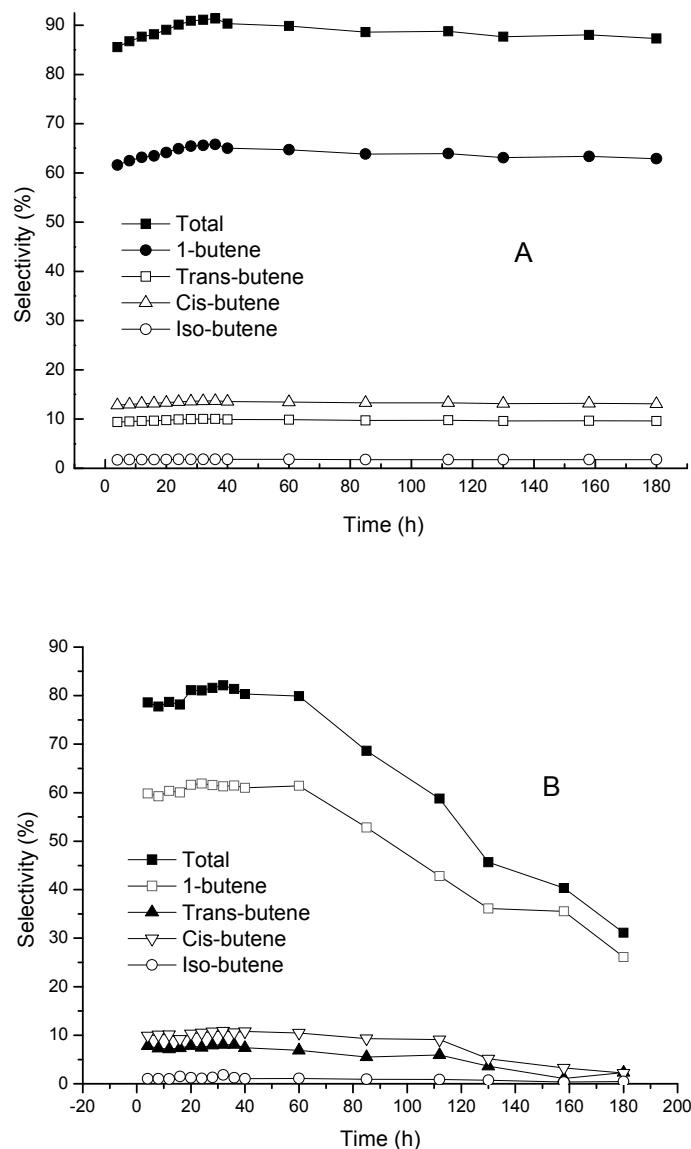


**Figure 7.** Dehydration of 1-butanol under optimal conditions ( $375.78\text{ }^{\circ}\text{C}$  and  $1.67\text{ h}^{-1}$  of WHSV) (A): Zn-Mn-Co modified  $\gamma$ -Al<sub>2</sub>O<sub>3</sub>. (B): Unmodified  $\gamma$ -Al<sub>2</sub>O<sub>3</sub>.

### 3. Materials and Methods

#### 3.1. Materials

The pseudo-boehmite was provided by the Catalyst Plant of Nankai University, Tianjin, China.

#### 3.2. Catalyst Preparation

The catalysts tested in this study were  $\gamma$ -Al<sub>2</sub>O<sub>3</sub> and Zn-Mn-Co/ $\gamma$ -Al<sub>2</sub>O<sub>3</sub>. Pseudo-boehmite was converted to  $\gamma$ -Al<sub>2</sub>O<sub>3</sub> after being calcined at  $600\text{ }^{\circ}\text{C}$  for 5 h. One hundred milliliters of a solution containing 1% Zn(NO<sub>3</sub>)<sub>2</sub>, 4% Mn(NO<sub>3</sub>)<sub>2</sub>, and 3% Co(NO<sub>3</sub>)<sub>2</sub> was added to 10 g  $\gamma$ -Al<sub>2</sub>O<sub>3</sub> with continuous stirring. The resulting solution was placed in an autoclave and treated at  $150\text{ }^{\circ}\text{C}$  for 4 h. The treated  $\gamma$ -Al<sub>2</sub>O<sub>3</sub> was washed with distilled water, then dried at  $120\text{ }^{\circ}\text{C}$  for 12 h, and calcined at  $600\text{ }^{\circ}\text{C}$  in air for 5 h. The resultant powder was molded under 20 MPa pressure to tablets, which were then crushed into particles and sieved to size 20–40 mesh.

### 3.3. Experimental Design

The interaction effects of reaction temperature and WHSV on 1-butanol dehydration were investigated by response surface methodology (RSM). The experimental scheme in this study was designed by Design-Expert 8.0.5 Trial. The catalytic performance was evaluated using the butene yield. In order to express the effect of factors including reaction temperature and WHSV on the dependent variable ( $Y$ ), the responses were fitted by the regression model expressed in Equation (2). The optimal point was predicted by a quadratic model, which was expressed as:

$$Y = b_0 + \sum b_i x_i + \sum b_{ii} x_i^2 + \sum b_{ij} x_i x_j \quad (2)$$

$i = 1, 2, \dots, k; j = 1, 2, \dots, k; i \neq j,$

where  $Y$  is the predicted response,  $x_i$  and  $x_j$  are independent variables,  $b_0$  is the intercept,  $b_i$  is the linear coefficient,  $b_{ii}$  is the quadratic coefficient, and  $b_{ij}$  is the interaction coefficient.

The experiments were performed in accordance with the conditions listed in Table 7, which were designed by a central composite design. The experimental data were used to calculate the second-order polynomial coefficients, and the model was evaluated by the analysis of variance (ANOVA) technique in the Design-Expert 8.0.5 Trial. The coefficient of determination  $R^2$  was used to evaluate the quality of the fit of the polynomial model equation. F-test and  $t$ -test were used to check the statistical and regression coefficient significance.

### 3.4. 1-Butanol Dehydration Experiments

The experiments on the catalytic dehydration of 1-butanol were performed in a micro-reactor device (Figure 8). First, 1.3 g 20–40 mesh catalyst was loaded in the middle of a reactive tube, fixed bed reactor (440 mm length, 8 mm I.D.), and the space under the catalyst bed in the reactor was filled with ceramic chips. The catalyst was pretreated at 450 °C in  $N_2$  for 1 h and then cooled to the test temperature. The feed rate of 620 g/L 1-butanol solution was controlled by a micro peristaltic pump, and the 1-butanol was vaporized by a vaporizer.

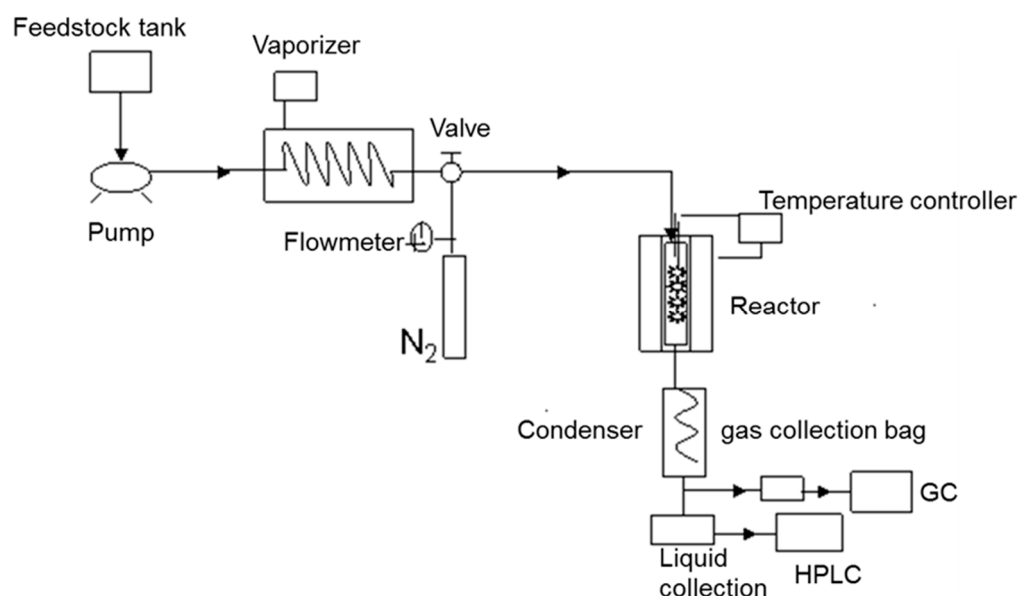


Figure 8. Apparatus for butanol dehydration.

### 3.5. Analytical Methods

The analysis of gas phase products was performed on Shimadzu-2010 gas chromatograph (Shimadzu, Kyoto, Japan) equipped with a flame ionization detector (FID), and the components in the product were separated by a capillary column (Alumina/ $NaSO_4$ , 30 mm  $\times$  0.5 mm  $\times$  10  $\mu$ m)

with nitrogen (pressure 60 kPa) as the carrier gas. The temperatures of the injector and detector were maintained at 150 °C and 250 °C, respectively. The temperature of the column oven was programmed to initially remain at 100 °C for 2 min, then rise to 113 °C at a rate of 10 °C/min, and finally reach 153 °C at a rate of 20 °C/min and remain at that temperature for 2.7 min. The flow rates of hydrogen and air were 40 and 400 mL/min, respectively.

HPLC (Shimadzu LC 20A, Kyoto, Japan) equipped with a refractive index detector and an Aminex HPX-87H column was used to analyze the liquid products. The compound 1-Butanol was analyzed at 65 °C with 5 mM H<sub>2</sub>SO<sub>4</sub> as the mobile phase at 0.8 mL/min.

### 3.6. Catalyst Characterization

Polymorphs of the catalysts were characterized by an X-ray diffraction system using a D8 Advance instrument (Bruker, Karlsruhe, Germany). The X-ray wavelength was 1.5406 Å, and the step size was 0.01°. The voltage and current were 40 KV and 40 mA, respectively. The scan speed and the scan range were 0.1 s/step and 10–80°, respectively.

The specific surface areas and porosity of the catalysts were examined using Tristar 3020 II (Micromeritics, Norcross, GA, USA), and the structural parameters were determined by the BET method. Nitrogen was used as the gas adsorbate at 77 K.

The acid strength of the catalysts was measured by the Py-TPD method with an Autochem II2920 (Micromeritics, Norcross, GA, USA). The acidity measurements were carried out by pyridine adsorption IR spectra with Nicolet 6700. The powder samples were molded to thin wafers (~20 mg) and then placed in a treatment cell for 2 h, where the temperature was raised to 500 °C, and in a high vacuum with  $1.0 \times 10^{-3}$  Pa.

The metal loadings of the modified catalysts were measured by ICP-AES with VISTA-MPX (Varian, Palo Alto, CA, USA).

## 4. Conclusions

The dehydration of 1-butanol to butenes is a major step in the process of converting 1-butanol to jet fuel and accounts for a significant portion of the total costs. An efficient and economic catalytic dehydration process was developed in this study. A high-concentration 1-butanol solution was used as feedstock, which was more consistent with the concentration of butanol from fermentation. Zn-Mn-Co modified  $\gamma$ -Al<sub>2</sub>O<sub>3</sub> was prepared, and the catalytic performance of the catalysts in 1-butanol dehydration to butenes was investigated. The catalytic performance of Zn-Mn-Co/ $\gamma$ -Al<sub>2</sub>O<sub>3</sub> was superior to that of unmodified  $\gamma$ -Al<sub>2</sub>O<sub>3</sub> at different reaction temperatures and WHSV. The reaction temperature and WHSV were optimized by RSM, and, at the optimal conditions, (375 °C and a WHSV of 1.67 h<sup>-1</sup>), the total selectivity of butene achieved 90%, and the conversion rate of 1-butanol reached 100%, which were 10% and 6% higher than those obtained using unmodified  $\gamma$ -Al<sub>2</sub>O<sub>3</sub>. According to the results of characterization, the loading amounts of zinc, manganese, and cobalt were 0.54%, 0.44%, and 0.23%, respectively, and the crystallinity and acidity of  $\gamma$ -Al<sub>2</sub>O<sub>3</sub> were enhanced after the modification. These results provide a theoretical basis for the further optimization of bio-jet fuel production with a high concentration of 1-butanol.

**Author Contributions:** Methodology, K.-K.C. and J.-A.Z.; software, H.-J.L.; formal analysis, X.Y. and Y.-J.Z.; investigation, J.W.; data curation, Z.-N.L. and S.M.; writing—original draft preparation, J.W.; writing—review and editing, J.W., K.-K.C. and J.-A.Z.; supervision, K.-K.C. and J.-A.Z.; project administration, J.-A.Z.; funding acquisition, J.-A.Z.

**Acknowledgments:** This research was funded by the National Key R&D Program of China (No. 2016YFE0131300), the project of NSFC-NRCT (No. 51861145103), the Boeing Company (No. 2015-156), and the Foundation of Key Laboratory for Industrial Biocatalysis (Tsinghua University), Ministry of Education (No. 2015302).

**Conflicts of Interest:** The authors declare no conflict of interest.

## References

1. Chiamonti, D.; Prussi, M.; Buffi, M.; Tacconi, D. Sustainable bio kerosene: Process routes and industrial demonstration activities in aviation biofuels. *Appl. Energy* **2014**, *136*, 767–774. [[CrossRef](#)]
2. Danilo, S.B.; Adriano, P.M. Jet fuel production in eucalyptus pulp mills: Economics and carbon footprint of ethanol vs. butanol pathway. *Bioresour. Technol.* **2018**, *268*, 9–19.
3. Zhang, W.L.; Liu, Z.Y.; Liu, Z.; Li, F.L. Butanol production from corncob residue using *Clostridium beijerinckii* NCIMB 8052. *Lett. Appl. Microbiol.* **2012**, *55*, 240–246. [[CrossRef](#)]
4. Ujor, V.; Agu, C.V.; Gopalan, V.; Ezeji, T.C. Allopurinol-mediated lignocellulose-derived microbial inhibitor tolerance by *Clostridium beijerinckii* during acetone-butanol-ethanol (ABE) fermentation. *Appl. Microbiol. Biotechnol.* **2015**, *99*, 3729–3740. [[CrossRef](#)] [[PubMed](#)]
5. Lin, Z.N.; Liu, H.J.; Yan, X.; Zhou, Y.J.; Cheng, K.K.; Zhang, J.A. High-efficiency acetone-butanol-ethanol production and recovery in non-strict anaerobic gas-stripping fed-batch fermentation. *Appl. Microbiol. Biotechnol.* **2017**, *101*, 8029–8039. [[CrossRef](#)] [[PubMed](#)]
6. Xue, C.; Zhao, J.B.; Liu, F.F.; Lu, C.C.; Yang, S.T.; Bai, F.W. Two-stage in situ gas stripping for enhanced butanol fermentation and energy-saving product recovery. *Bioresour. Technol.* **2013**, *135*, 396–402. [[CrossRef](#)] [[PubMed](#)]
7. Xue, C.; Du, G.Q.; Sun, J.X.; Chen, L.J.; Gao, S.S.; Yu, M.L.; Yang, S.T.; Bai, F.W. Characterization of gas stripping and its integration with acetone-butanol-ethanol fermentation for high-efficient butanol production and recovery. *Biochem. Eng. J.* **2014**, *83*, 55–61. [[CrossRef](#)]
8. West, R.M.; Braden, D.J.; Dumesic, J.A. Production of alkanes from biomass derived carbohydrates on bi-functional catalysts employing niobium-based supports. *J. Catal.* **2009**, *10*, 1743–1746. [[CrossRef](#)]
9. Sun, H.; Blass, S.; Michor, E.; Schmidt, L. Autothermal reforming of butanol to butenes in a staged millisecond reactor: Effect of catalysts and isomers. *Appl. Catal. A Gen.* **2012**, *445–446*, 35–41. [[CrossRef](#)]
10. Sedjame, H.J.; Lafaye, G.; Barbier, J., Jr. N-butanol removal over alumina supported platinum catalysts. *Appl. Catal. B Environ.* **2013**, *132–133*, 132–141. [[CrossRef](#)]
11. Zhang, D.; Alhajri, R.; Barri, S.A.; Chadwick, D. One-step dehydration and isomerisation of n-butanol to iso-butene over zeolite catalysts. *Chem. Commun.* **2010**, *46*, 4088–4090. [[CrossRef](#)] [[PubMed](#)]
12. Macho, V.; Jurecekova, E.; Hudec, J. Dehydration of C4 alkanols conjugated with a positional and skeletal isomerisation of the formed C4 alkenes. *Appl. Catal. A Gen.* **2001**, *214*, 251–257. [[CrossRef](#)]
13. Wang, L.; Chen, H.Z. Increased fermentability of enzymatically hydrolyzed steam-exploded corn stover for butanol production by removal of fermentation inhibitors. *Process Biochem.* **2001**, *46*, 604–607. [[CrossRef](#)]
14. Nahreen, S.; Gupta, R.B. Conversion of the acetone-butanol-ethanol (ABE) mixture to hydrocarbons by catalytic dehydration. *Eenergy Fuel* **2013**, *27*, 2116–2125. [[CrossRef](#)]
15. Lopez-Pedrajas, S.; Estevez, R.; Schnee, J.; Schnee, J.; Gaigneaux, E.M.; Luna, D.; Bautista, F.M. Study of the gas-phase glycerol oxidehydration on systems based on transition metals (Co, Fe, V) and aluminium phosphate. *Mol. Catal.* **2018**, *455*, 68–77. [[CrossRef](#)]
16. Popa, A.; Sasca, V.; Verdes, O.; Oszko, A. Preparation and catalytic properties of cobalt salts of Keggin type heteropolyacids supported on mesoporous silica. *Catal. Today* **2018**, *306*, 233–242. [[CrossRef](#)]
17. Armenta, M.A.; Valdez, R.; Silva-Rodrigo, R.; Olivias, A. Diisopropyl ether production via 2-propanol dehydration using supported iron oxides catalysts. *Fuel* **2019**, *236*, 934–941. [[CrossRef](#)]
18. Li, F.Y.; Liu, Z.Z.; Shen, D.J.; Zhang, M.H. Catalytic dehydration of ethanol to ethylene over nickel modified HZSM-5 catalysts. *Mod. Chem. Ind.* **2013**, *33*, 54–57.
19. Wang, W.; Cheng, K.K.; Xue, J.W.; Zhang, J.A. Optimization of ethylene production from ethanol dehydration using Zn-Mn-Co/HZSM-5 by response surface methodology. *Chin. J. Biotechnol.* **2011**, *27*, 412–418.
20. Osman, A.I.; Abu-Dahrieh, J.K.; Rooney, D.W.; Thompson, J.; Halawy, S.A.; Mohamed, M.A. Surface hydrophobicity and acidity effect on alumina catalyst in catalytic methanol dehydration reaction. *J. Chem. Technol. Biotechnol.* **2017**, *92*, 2952–2962. [[CrossRef](#)] [[PubMed](#)]
21. Said, E.A.A.; El-Wahab, M.M.M.A.; Abdelhak, M.M. The role of Brønsted acid site strength on the catalytic performance of phosphotungstic acid supported on nano  $\gamma$ -alumina catalysts for the dehydration of ethanol to diethyl ether. *React. Kinet. Mech. Catal.* **2017**, *122*, 1–17. [[CrossRef](#)]
22. Yu, F.; Zhang, M.H.; Ye, G. Influence of different metal ions on the rehydration properties of aluminas. *Acta Sini Pet Process Sect.* **1999**, *15*, 25–27.

23. Fei, J.H.; Yang, M.X.; Hou, Z.Y.; Zheng, X.M. Effect of the addition of manganese and zinc on the properties of copper-based catalyst for the synthesis of syngas to dimethyl ether. *Energy Fuel* **2004**, *18*, 1584–1587. [[CrossRef](#)]
24. Thommes, M.; Kaneko, K.; Neimark, A.V.; Olivier, J.P.; Rodriguez-Reinoso, F.; Rouquerol, J.; Sing, K.S.W. Physisorption of gases with special reference to the evaluation of surface area and pore size distribution (IUPAC Technical Report). *Pure Appl. Chem.* **2015**, *87*, 1051–1069. [[CrossRef](#)]
25. Phung, T.K.; Lagazzo, A.; Crespo, M.Á.R.; Escribano, V.S.; Busca, G.A. Study of commercial transition aluminas and of their catalytic activity in the dehydration of ethanol. *J. Catal.* **2014**, *311*, 102–113. [[CrossRef](#)]
26. Abattista, F.; Delmastro, S.; Gozzelino, G.; Mazza, D.; Vallino, M.; Busca, G.; Lorenzelli, V.; Ramis, G. Surface characterization of amorphous alumina and its crystallization products. *J. Catal.* **1989**, *117*, 42–51. [[CrossRef](#)]
27. Morterra, C.; Magnacca, G. A case study: Surface chemistry and surface structure of catalytic aluminas, as studied by vibrational spectroscopy of adsorbed species. *Catal. Today* **1996**, *27*, 497–532. [[CrossRef](#)]
28. Khabtou, S.; Chevreau, T.; Lavalley, J.C. Quantitative infrared study of the distinct acidic hydroxyl groups contained in modified Y zeolites. *Microporous Mater.* **1994**, *3*, 133–148. [[CrossRef](#)]
29. Zheng, H.D.; Lin, Y.; Wang, M.C.; Liu, J.; Wu, D.; Chen, J.J.; Yin, G.H.; Oyama, S.T.; Zhao, S.Y. The influence of solvent polarity on the dehydrogenation of isoborneol over a Cu/ZnO/Al<sub>2</sub>O<sub>3</sub> catalyst. *Catal. Today* **2019**, *323*, 44–53. [[CrossRef](#)]
30. Ashour, S.S. Factors Affecting the Activity and Selectivity of Alumina Catalysts in the Dehydration of 1-Butanol. *Adsorpt. Sci. Technol.* **2004**, *22*, 475–483. [[CrossRef](#)]
31. El-Molla, S.A. Surface and catalytic properties of Cr<sub>2</sub>O<sub>3</sub>/MgO system doped with manganese and cobalt oxides. *Appl. Catal. A Gen.* **2005**, *280*, 189–197. [[CrossRef](#)]
32. Li, G.; Liu, Y.; Tang, Z.; Liu, C.G. Effects of rehydration of alumina on its structural properties, surface acidity, and HDN activity of quinoline. *Appl. Catal. A Gen.* **2012**, *437–438*, 79–89. [[CrossRef](#)]



© 2019 by the authors. Licensee MDPI, Basel, Switzerland. This article is an open access article distributed under the terms and conditions of the Creative Commons Attribution (CC BY) license (<http://creativecommons.org/licenses/by/4.0/>).